https://doi.org/10.2352/EI.2023.35.15.COLOR-190

Estimation of the fluorescence emission spectrum of dental composite resin samples of varying thickness

Vincent Duveiller[1,], Arthur Gautheron[1], Anthony Cazier[1], Lionel Simonot[2], Raphaël Clerc[1], Jean-Pierre Salomon[3,4,5,6], Mathieu Hébert[1]*

[1]Université Jean Monnet Saint-Etienne, CNRS, Institut d Optique Graduate School, Laboratoire Hubert Curien UMR 5516, F-42023 SAINT-ETIENNE, France; [2]Université de Poitiers, Institut Pprime CNRS, Chasseneuil Futuroscope, France; [3]Faculté d'Odontologie de Nancy, Département des Dispositifs Médicaux et Biomatériaux Dentaires, Université de Lorraine, France; [4]Institut de Science des Matériaux de Mulhouse UMR 7361 CNRS, Université de Haute Alsace, France ; [5]Université de Strasbourg, France; [6]Department of Restorative Dentistry, Division of Biomaterials and Biomechanics. Oregon Health and Science University, Portland, Oregon, USA
**vincent.duveiller@institutoptique.fr*

Abstract

The fluorescence property of human teeth under UV light has long been studied in dentistry and is now used in the diagnosis of anomalies, such as dental decays. Its role in the appearance of teeth and dental restorations has also been demonstrated, and fluorescence, even under daylight, may sensibly modify the appearance of dental restorations. As such, dental resin composites used in aesthetic restorative dentistry include fluorescent agents which aim to imitate the natural fluorescence of teeth. While several studies have measured the fluorescence properties of dental biomaterials and a few other studies have focused on predicting the color of samples, the influence of fluorescence on color prediction models remains to be assessed. In this paper, we propose a prediction model for the spectral emission of slices of a dental biomaterial as a function of their thickness, in reflection and in transmission modes, with the aim of improving color prediction models for these materials.

Introduction

The fluorescence of enamel and dentine under UV light, and even under visible light, has first been described in the early 1920s [1]. Several studies have emphasized the importance of reproducing the fluorescence of natural teeth in the fabrication of dental restorations in order to improve the aesthetic quality of the filling [2]. Furthermore, it has been shown that fluorescence under daylight has an influence on color parameters of dental resin composites [3].

In order to improve the esthetic quality of their biomaterials, dental resin composite manufacturers include fluorescent agents in their chemical composition with the aim to mimic the natural fluorescence of dental tissues. However, the fluorescence of natural human teeth is still not completely understood [4]. In particular, it seems that their fluorescence it caused by a combination of several fluorescence agents [5]. Because of this complexity, material manufacturers are still not able to fully reproduce the natural fluorescence of teeth [6].

In order to study the fluorescence of enamel, dentine, or dental biomaterials, several techniques have been proposed in the literature. The fluorescent spectrum of samples was observed with methods based on a photographic camera under UV light [7] or daylight [3], or with a spectrophotometer [8]. In other studies, a spectrofluorometer was used in order to measure the fluorescence emission spectrum for different excitation wavelengths, thus creating bi-spectral plots showing the fluorescence emission as a function of the excitation wavelength [9].

Several studies have shown how optical models can predict the color of dental restorations in specific cases [10-14]. Despite a good prediction performance in some cases, the accuracy of optical models is undermined by fluorescence as dental materials are fluorescent in the visible domain and the emission by fluorescence is mixed with the reflection and transmission of light. In this case, fluorescence effects are incorporated into the spectral values of optical parameters of the models even though they are not taken into account explicitly: in consequence, they are falsely interpreted as absorption or scattering. Thus, it would be possible to improve the accuracy of spectral reflectance/transmittance prediction models for slices of dental biomaterials by accounting for the fluorescence phenomenon. Such a method would also enable to predict the color of samples of dental resin composites observed under UV light.

Therefore, the aim of this study is to predict the spectral fluorescence emission of slices of a flowable resin composite with respect to their thickness. Our research hypotheses are that spectral exitance of a slice of material, different at the two sides of the slice ("reflection" and "transmission" modes), varies according to the excitation wavelength and that its amplitude varies with respect to the thickness of the sample. To verify these hypotheses, we use a set of samples of varying thickness of one dental resin composite, and measure the spectral fluorescence exitance of each sample under a near UV light source in reflectance mode and in transmittance mode. A two-flux model extended to fluorescence [15] is used to predict the amplitude of the peak of fluorescence for each measurement. This model requires coefficients describing the absorption and scattering of light for both the excitation wavelengths (near-UV) and emission wavelengths, which will be determined be means of a state-of-the-art two-flux model [13] calibrated from measurements performed with a spectrophotometer under white light.

Set of samples investigated

Samples of the Estelite Universal Flow Medium in A2 shade (Tokuyama Company) were considered for this study. In the Vita Classical colorimetric terminology of dental resin composites, the A2 shade is a light color with low chroma level, which aims to replace enamel. Estelite Universal Flow is a direct light cured supra-nano filled resin composite which contains spherical silica-zirconia filler (mean particle size: 200 nm), bis-GMA, Bis-MPEPP, TEGDMA, UDMA, Mequinol, Dibutyl hydroxyl toluene, and UV absorber. Batch number was 0503.

Eight flat cylindrical samples with different thicknesses were fabricated. The flowable dental resin was injected between two glass-slides, whose spacing is controlled with high precision wedges and defines the nominal thickness of the sample. Samples with thickness 0.4 mm, 0.5 mm, 0.8 mm, 1.0 mm, 1.2 mm, 1.5 mm, 1.6 mm, and 2.0 mm were made. The samples were light-cured with a LED light-curing unit (Radii Xpert, SDI company at 1500 mW/cm^2) according to the curing scheme I.S.O. 4049:2009 [16] (each sample

was irradiated five times, 40 seconds each irradiation, at 12-3-6-9 o'clock positions and ending in the center of the sample). The sample diameter, determined by the volume of material deposited, is ranging from 20 mm to 22 mm. The thickness of each sample after curing was measured with a precision micrometer as resin composites shrink during the curing process. Although the measured thicknesses were considered in the experiments, samples will be referred to by their nominal thickness for clarity. The fabricated samples are presented on Fig. 1. The measured thickness of each sample is given in Table 1.

Figure 1: Samples of the Estelite Universal Flow Medium material shade A2 on a drawdown card (no optical contact). The picture is taken in daylight with an uncalibrated camera. Samples are sorted from the thickest on the left to the thinnest on the right: 2.0 mm, 1.6 mm, 1.5 mm, 1.2 mm, 1.0 mm, 0.8 mm, 0.5 mm and 0.4 mm.

Table 1: Measured thickness of samples.

Nominal thickness (in mm)	Measured thickness (in mm)
0.4	0.352
0.5	0.497
0.8	0.757
1.0	0.960
1.2	1.138
1.5	1.416
1.6	1.518
2.0	1.934

Measuring the fluorescence emission spectrum

The reflectance and transmittance factors of each sample were measured with a commercial spectrophotometer based on white light accepting or cutting UV. In addition, an optical bench was designed to measure the spectral exitance of samples due to fluorescence alone, both on the illuminated side ("reflectance mode") and on the opposite side ("transmittance mode"), with monochromatic light sources (lasers at 380 nm and 405 nm). These measurement setups are presented in detail below, as well as the analysis of the measurements obtained.

Measurements with the spectrophotometer

We used the Color i7 from X-Rite, based on white light including some UV to measure the samples' spectral reflectance and transmittance factors. It includes an integrating sphere with a Xenon pulsed light for illumination and the sensor captures the exiting radiance at 8° from the sample normal in reflectance mode and along the normal direction in transmittance mode (respectively, d:8° and d:0° measuring geometry as recommended by the CIE [17]). The largest available illumination aperture of 17 mm was selected, while the smallest measuring aperture of 6 mm was selected in order to limit the edge-loss phenomenon, which is known to alter the measurement of translucent materials [18,19]. In reflectance mode, the specular component is included in the measurements. This spectrophotometer allows to place a UV filter blocking light below 400 nm (*UV-excluded* measurement), or to remove the filter to accept UV light from 360 nm (*UV-included* measurement). In the latter mode, the spectrophotometer is calibrated with a specific fluorescent calibration standard in order to reproduce the L* value of the calibration standard under the D65 illuminant. Thus, each reflectance and transmittance measurement were performed in the UV-excluded mode and the UV-included mode without any support behind the samples, in a completely dark room. Each measurement was repeated 7 times and the average for each measurement is shown in Fig. 2a. The difference between measurements in UV-included and UV-excluded modes is shown in Fig. 2b.

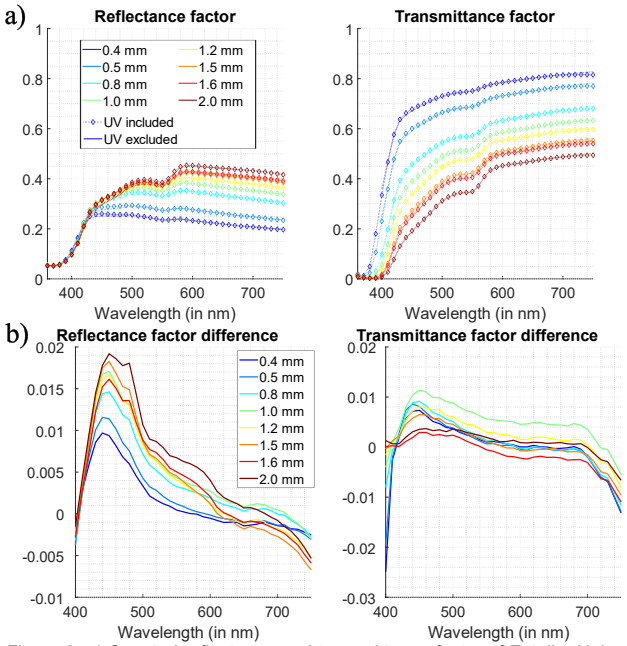

Figure 2: a) Spectral reflectance and transmittance factor of Estelite Universal Flow Medium A2 samples with specified thickness. b) Difference between measurements in the UV-included and UV-excluded mode.

The sample of thickness 1.2 mm is used as a calibration sample, which means that its reflectance and transmittance factors are used to estimate the absorption and scattering parameters of the material for the excitation and emission wavelengths according to a two-flux model. These coefficients are necessary to predict the amplitude of the fluorescence peak with the fluorescence two-flux model.

Table 2: L*a*b* color coordinates of samples measured with the Color i7 spectrophotometer in UV-included and UV-excluded modes and CIEDE2000 color distance between measurements in both modes.

Nominal thickness (in mm)	UV-included			UV-excluded			
	L*	a*	b*	L*	a*	b*	ΔE_{00}
0.4	56.05	-1.57	-2.20	55.97	-1.74	-1.10	1.06
0.5	59.89	-2.00	0.18	59.76	-2.15	1.36	1.13
0.8	65.11	-2.14	5.15	64.81	-2.23	6.39	1.02
1.0	66.94	-1.72	7.30	66.58	-1.81	8.72	1.08
1.2	68.09	-1.55	9.46	67.78	-1.51	10.91	1.04
1.5	69.00	-0.90	10.68	68.69	-0.83	12.30	1.11
1.6	69.20	-0.83	11.40	68.84	-0.66	12.72	0.94
2.0	70.28	-0.20	13.01	69.80	-0.10	14.57	1.04

The L*a*b* color coordinates for each measurement are calculated by using the color matching functions established with a

2° standard observer, the D65 power spectral distribution as illuminant [20] and a perfectly white diffuser (reflectance factor equal to 1) as reference for the chromatic adaptation. The L*a*b* color coordinates and color distance between UV-included and UV-excluded measurements are presented in Table 2.

Measurements: 380 nm light source

An optical bench was designed using a 380 nm fiber injected laser diode source (LBX-375-200-HPE-PPA from Oxxius) with a diaphragm enabling to tune the size of the beam for illumination samples (excitation signal at 380 nm). The tunable output power of the laser was set very low to minimize non-linear effects. Samples were placed on a sample holder at approx. 15 cm from the laser. A fiber spectrophotometer (QEPro from OceanInsight with a round-to-linear fiber bundle PL200-2-UV-VIS from OceanInsight) was placed behind the sample at an approx. 15 cm distance in a 0°:0° geometry in transmittance mode and in a 0°:20° geometry in reflectance mode. A lens was used to control the measuring aperture of the spectrophotometer on the sample. The diaphragm on the laser source was set so that only a small spot hits the center of the sample, while the lens on the spectrophotometer was set so that it collects light emerging from the whole area of the sample. The experimental setup is similar to the setup presented on Fig. 4 for measurements with a 405 nm light source. The integration time of the sensor was set to 60 seconds (the emittance of the samples being low with the selected irradiance of the samples). Each acquisition was performed 5 times and the average was calculated. Because of the high spectral resolution of the spectrophotometer (0.4 nm), a rolling average was then calculated for each measurement, which are presented on Fig. 3a while the peak of fluorescence with respect to the sample thickness is presented on Fig. 3b.

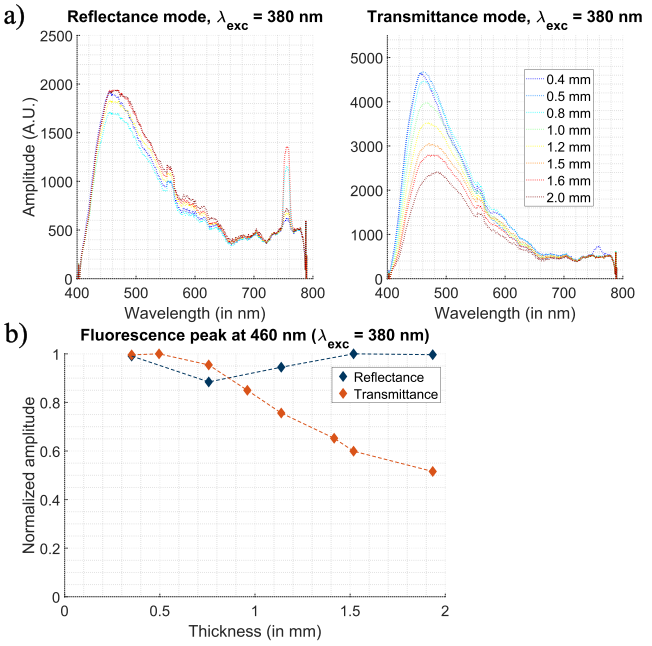

Figure 3: a) Average fluorescence spectrum in reflectance and transmittance modes of the samples with different thicknesses under a 380 nm light source. A peak visible at 760 nm is the 2nd order emission of the laser and does not result from samples' fluorescence. b) Fluorescence peak in reflectance mode and transmittance mode with respect to sample thickness.

The fluorescence signal measured in reflectance mode is almost the same for all samples: the spectral shape is similar. We also observe that the amplitude is nearly constant. It is probable that the excitation beam at 380 nm is totally attenuated across the thinnest sample (400 µm). Consequently, no more flux is emitted within thicker samples and the exitance at the side of the incident beam (reflectance mode) remains the same for all the samples. At the other side, the exitance decreases if the sample thickness increases because the light emitted in the first 400 µm of the sample must cross the rest of the sample's volume where it is attenuated by absorption and backscattering.

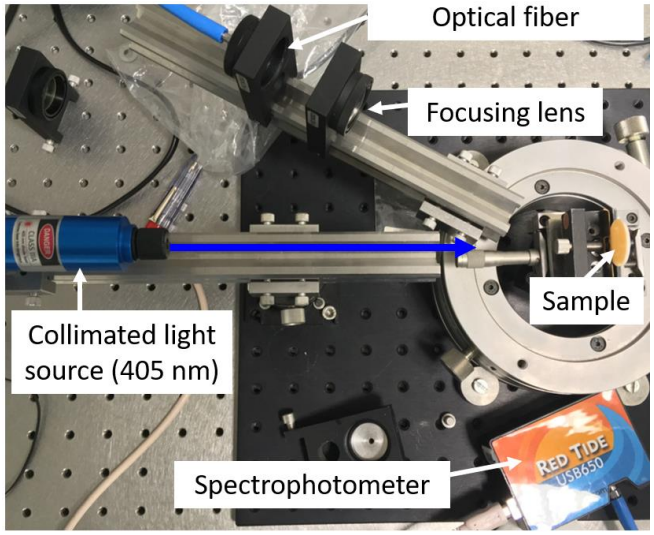

Figure 4: Optical setup used to measure the fluorescence spectrum in reflectance and transmittance mode. The optical fiber collects light exiting from the samples and directs it to the spectrophotometer. A rotatable arm enables to easily switch between the reflectance and transmittance configurations.

Measurements: 405 nm light source

An optical setup similar to the one used for illuminating the samples at 380 nm was made to illuminate them at 405 nm. The setup is presented on Fig. 4. The light source used for excitation is a laser diode emitting light at 405 nm commercialized by DidaConcept with a focusing lens enabling to focus the laser spot in the center of the sample. The fiber spectrophotometer used is a Red Tide USB650 commercialized by OceanOptics. A focusing lens ensures that the spectrophotometer captures light emerging from the whole surface of the sample. The measuring geometry was 0°:25° in reflectance mode and 0°:0° in transmittance mode.

The integration time for measurements was ranging from 400 ms to 500 ms depending on the thickness of the sample, and each measurement was the average of 10 acquisitions. Measurements are presented on Fig. 5a. This measuring process was repeated 5 times in order to evaluate the repeatability of measurements and the average of the fluorescence peak with respect to the sample thickness is presented on Fig. 5b.

The amplitude of the fluorescence signal in reflectance mode varies with the sample thickness; it increases before reaching a plateau for samples thicker than 1.0 mm. This hints that the absorbance of the material at 405 nm might be lower than at 380 nm, and light travels deeper inside the layer, until about 1 mm. Therefore, the fluorescence signal measured in reflectance and transmittance modes increases from 0.4 to 1.0 mm as more fluorophores are excited and emit fluorescence. Beyond 1.0 mm, the excitation signal is totally absorbed and the signal in reflectance mode reaches a plateau while the signal in transmittance mode is

attenuated by absorption and backscattering (as with an excitation at 380 nm).

For a given light source and an observation mode (reflectance or transmittance mode), the shape of the fluorescence signal is very similar with respect to the sample thickness. Small variations can be observed and are probably due to absorption and scattering of the fluorescence signal by the resin composite, which increases with the sample thickness. It is reasonable to assume that the shape is constant with respect to the sample thickness, at least in the range of thicknesses tested, and that it is therefore sufficient to predict exitance at the wavelength where the spectrum is maximal (amplitude of the peak of fluorescence) to predict the whole spectral exitance in each mode. The peak of fluorescence is at 460 nm for an excitation light source at 380 nm, and at 495 nm for an excitation light source at 405 nm.

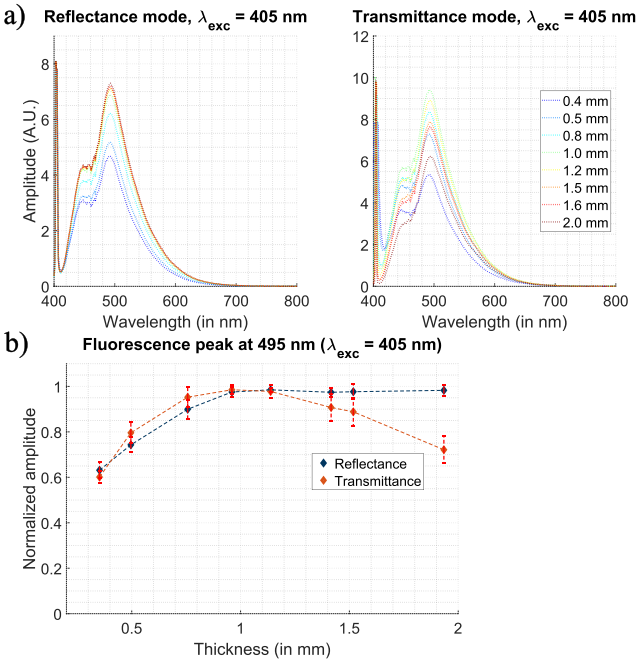

Figure 5: a) Average fluorescence spectrum in reflectance and transmittance modes of samples under a 405 nm light source. b) Fluorescence peak in reflectance mode and transmittance mode with respect to sample thickness.

Optical model for fluorescence

In order to predict the spectral exitance of the samples for a given excitation wavelength, we implemented a two-flux model accounting for fluorescence, as proposed by Simonot *et al.* [15].

In addition to modeling the propagation of light within a turbid medium, like the state of the art two-flux model [21,22], this approach describes the propagation of light emitted by fluorescence at any depth within the material, resulting from absorption at an excitation wavelength. The exitance due to fluorescence therefore contributes to the reflectance and transmittance of the material. The propagation of the excitation signal is described by a Kubelka-Munk system of differential equations based on absorption and scattering coefficients K_a and S_a, respectively. A portion of the excitation signal that is absorbed is re-emitted at longer wavelengths. The propagation of the light re-emitted is then described by another Kubelka-Munk system of differential equations, based on the absorption and scattering coefficients K_e and S_e respectively. Formulae are then derived by solving the system of differential equations for the reflectance and transmittance of the medium accounting for the fluorescence emission, assumed to be angularly isotropic. Therefore, the same amount of fluorescence is emitted forwards and backwards. The model depends on the parameters K_a, S_a, K_e, S_e, as well as F, the intrinsic normalized fluorescence spectral distribution, and ϕ, the luminescent quantum efficiency of the medium.

Calibration of the fluorescence model

The six parameters listed above of the two-flux model extended to fluorescence are unknown. In the general case, the reflectance and transmittance factors are measured using a spectral broadband illumination, as it is the case with the Color i7 spectrophotometer, preventing to distinguish excitation signals from fluorescence emission signals. Therefore, the two-flux model extended to fluorescence can only be used when the wavelength of the excitation signal does not overlap with wavelengths of the emission signal, as is the case for our optical benches used for measuring the fluorescence emission with an incident signal at 380 nm or 405 nm.

In the latter case, the absorption (K_a) and scattering (S_a) parameters for the excitation signal can be extracted from reflectance and transmittance factor measurements performed with a spectrophotometer using a state-of-the-art two-flux model, as described in [13,14]. In the case where the wavelength of the excitation signal is 380 nm, UV-included measurements must be used to extract the K_a and S_a parameters, as the UV filter blocks light below 400 nm. However, for the excitation signal of 405 nm, UV-excluded measurements must be used to extract the K_a and S_a parameters. Indeed, the fluorescence emission signal resulting from an excitation signal at 380 nm is not negligible at 405 nm. Therefore, using UV-included measurements would cause K_a and S_a parameters extracted at 405 nm to incorporate some fluorescence signal resulting from excitation at lower wavelengths. Furthermore, it is highly likely that the samples investigated are fluorescent at 360 nm, which means that a fraction of K_a(380 nm) and S_a(380 nm) incorporates fluorescence, which is a limitation of our approach.

The absorption and scattering parameters for the fluorescence signal, namely K_e and S_e, can be derived from measurements performed with a spectrophotometer with a UV-excluded mode. Ideally, these parameters should be extracted from measurements in which the fluorescence phenomenon is absent, but this could not be done with the dental resin composite under study as it is fluorescent even at wavelengths longer than 420 nm. This approximation is mitigated by the fact that intensity of the fluorescence signal is much lower than the intensity of the reflected or transmitted signal.

The normalized fluorescence spectral distribution F and the luminescent quantum efficiency ϕ of the medium are unknown in the general case. However, when the fluorescence peak signal is considered, F is equal to 1, which leaves only ϕ to be fitted numerically.

Saunderson correction

The shift of refractive index between the material and its surrounding medium (air) at the interface refracts and reflects light according to Snell's laws and Fresnel formulae. This phenomenon is accounted for by the Saunderson correction [23], assuming that the interfaces are optically flat and smooth (which is the case of our samples). The Saunderson correction gives the reflectance and transmittance factors as measured with a spectrophotometer, denoted R and T respectively, as functions of the intrinsic reflectance and transmittance of the layer denoted ρ and τ respectively, being derived from the two-flux model according to formulae (1) and (2).

$$R = r_e + T_{in}T_{out}\frac{\rho - r_i(\rho^2 - \tau^2)}{(1 - r_i\rho)^2 - r_i^2\tau^2} \quad (1)$$

and

$$T = \frac{T'_{in}T'_{out}\tau}{(1 - r_i\rho)^2 - r_i^2\tau^2} \quad (2)$$

where the terms r_e, r_i, T_{in}, T_{out}, T'_{in} and T'_{out} denote the flux transfers at the interfaces by taking into account the measuring geometry. T'_{in} and T'_{out} refer to the lower interface while T_{in} and T_{out} refer to the upper interface with respect to the incident illumination. r_e and r_i are assumed equal at both interfaces (the latter assumption is discussed in details in [24]).

The r_i parameter of the Saunderson correction denotes the internal reflectance of the material-air interface. Its definition, based on angular radiance distribution function $L_i(\theta)$ is given in formula (3):

$$r_i = \int_{\theta=0}^{\pi/2} R_{21}(\theta)L_i(\theta)\sin(2\theta)d\theta \Big/ \int_{\theta=0}^{\pi/2} L_i(\theta)\sin(2\theta)d\theta \quad (3)$$

where $R_{21}(\theta)$ denotes the Fresnel angular reflectance of the interface at the side of the medium with highest optical index.

For a refractive index of 1.5, if the incident light is perfectly diffuse, i.e., $L_i(\theta)$ is a constant with respect to the angle, r_i = 0.6. However, we have already observed in [13,14] that this assumption does not hold for dental materials measured with a directional-hemispherical measuring geometry, unless a Lambertian background is placed behind the samples, in optical contact. Thin samples of dental materials are weakly scattering and thus the angular distribution of light cannot be assumed to be isotropic [24]. In the case of a transparent, non-scattering medium, the internal reflectance should take its specular value r_i = 0.04. We considered this value of 0.04 for the extraction of K_a, S_a, K_e and S_e parameters, assuming that the incident light is almost not scattered. However, fluorescence emission being isotropic, it is relevant to consider r_i = 60% in the two-flux model extended for fluorescence in order to predict the amplitude of the fluorescence peak.

Experimental verification

Let us compare the exitances measured with our setups and the ones predicted by the two-flux model extended to fluorescence at the wavelength corresponding to the peak of fluorescence: 460 nm for an excitation at 380 nm and 495 nm for an excitation at 405 nm.

For the propagation of the excitation light beam, the coefficients K_a(380 nm) and S_a(380 nm) are extracted from UV-included reflectance and transmittance factor measurements of the sample with thickness 1.2 mm (calibration sample) made with the Color i7, by means of an inverse two-flux model considering r_i = 4% in the Saunderson correction. K_a(405 nm), S_a(405 nm), K_e(460 nm), S_e(460 nm), K_e(495 nm) and S_e(495 nm) are extracted similarly, but from UV-excluded measurements. The normalized fluorescence emission spectrum F reaches its highest value for the fluorescence peak (460 nm under an incident light at 380 nm and 495 nm under an incident light at 405 nm). At this wavelength, we therefore assume that its value is 1. The luminescent quantum efficiency ϕ(460 nm) [resp. ϕ(495 nm)] is unknown and is therefore fitted to the fluorescence peak of measurements in reflectance mode and in transmittance mode with an excitation signal at 380 nm (resp. 405 nm).

Fluorescence peak prediction: 380 nm light source

The two-flux model extended to fluorescence is used to predict the fluorescence emission in reflectance and transmittance modes for thicknesses between 0.2 mm and 2.0 mm. According to the method described above, we find K_a(380 nm) = 4.6 mm^{-1}, S_a(380 nm) = 0.2 mm^{-1}, K_e(460 nm) = 0.4 mm^{-1}, S_e(460 nm) = 0.6 mm^{-1} and ϕ(460 nm) = 0.8. Because of geometric and radiometric issues in the measurements, the amplitude of the signals measured in reflectance mode are not comparable to the ones measured in transmittance mode. We therefore decided to represent them on a normalized scale, by setting the highest amplitude to 1 in each mode. The same normalization is applied to the predictions. The comparison between the measured and predicted amplitudes is shown in Fig. 6.

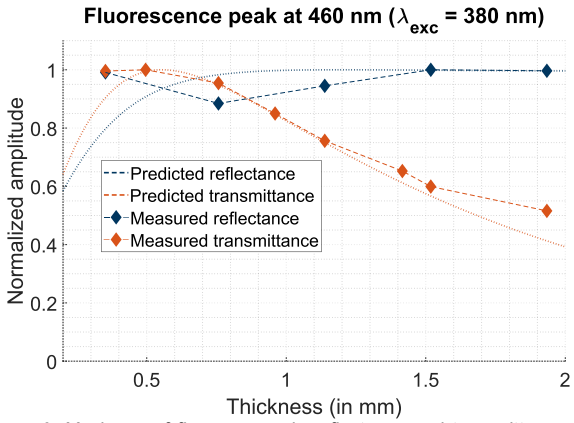

Figure 6: Maximum of fluorescence in reflectance and transmittance modes predicted by the two-flux extended model (solid lines) and measured (dashed lines). The excitation signal is at 380 nm and the peak of the emission signal is at 460 nm.

Within the limits of the measurement accuracy, the two-flux model extended to fluorescence seems fairly accurate in both reflectance and transmittance modes for predicting the fluorescence peak at 460 nm under a 380 nm excitation signal.

Fluorescence peak prediction: 405 nm light source

The two-flux model extended to fluorescence is used to predict the fluorescence emission in reflectance and in transmittance mode for thicknesses between 0.2 mm and 2.0 mm. According to the method described above, we find K_a(405 nm) = 2.0 mm^{-1}, S_a(405 nm) = 0.4 mm^{-1}, K_e(495 nm) = 0.2 mm^{-1}, S_e(495 nm) = 0.6 mm^{-1} and ϕ(495 nm) = 0.5. The same normalized scaling is used as for the excitation at 380 nm, for both the measured and predicted amplitudes shown in Fig. 7.

As for an excitation at 380 nm, the model predicts well the general evolution of the normalized peak amplitude as a function of the sample thickness with an excitation at 405 nm. This result is rather satisfying given the experimental conditions (low irradiances, fluctuations in time of laser sources, position of the samples, etc.) The slight difference of slope may be due to a small estimation error of the absorption and scattering coefficients, since they are computed from a simple two-flux model that does not take into account fluorescence and calibrated on one sample only (thickness of 1.2 mm).

There is thus floor for improvement, for example by improving the coefficient estimation method, or by using a monochromator for

the illumination of the sample: for each incident wavelength λ, the component emitted by fluorescence (at wavelengths larger than λ) could be distinguished from the reflected/transmitted component (at λ). Furthermore, the use of a spectrofluorometer would enable to extend this study to other wavelengths.

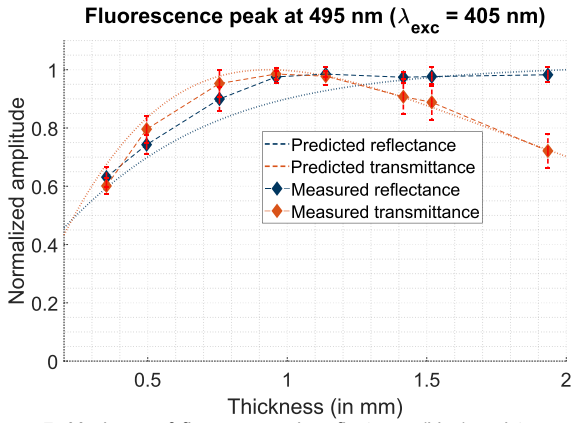

Figure 7: Maximum of fluorescence in reflectance (blue) and transmittance (orange) modes predicted by the two-flux extended model (solid lines) and measured (dashed lines). The excitation signal is at 405 nm and the peak of the emission signal is at 495 nm.

Conclusion

Despite measurements uncertainty and despite the known limitations of the two-flux model to capture light scattering in translucent, partially diffusing, materials, this work shows that the two-flux model extended to fluorescence enables to predict quite well the amplitude of the fluorescence peak in reflectance and transmittance modes with respect to the thickness of the sample evaluated, for a given excitation wavelength.

As we observed that the fluorescence spectrum is mostly independent on the sample thickness, this simple and efficient method also enables to predict for a given excitation wavelength the whole fluorescence spectrum in reflectance and transmittance modes.

To the best of our knowledge, this work is the first attempt at predicting the fluorescence signal of dental materials, and further work is underway to merge fluorescence prediction within more advanced reflectance and transmittance prediction models.

Acknowledgement

This work has been funded by a public grant from the French National Research Agency (ANR) under the "France 2030" investment plan, which has the reference EUR MANUTECH SLEIGHT - ANR-17-EURE-0026.

References

[1] Stübel H.: "Die Fluoreszenz tierischer Gewebe in ultraviolettem Licht," *Arch Ges Physiol*, vol. 142, pp. 1-14, 1921

[2] H. Filho, L. Maia, M. Araujo, and A. Ruellas, "Influence of optical properties of esthetic brackets (color, translucence, and fluorescence) on visual perception," Am J Orthod Dentofac. Orthop, vol. 141, pp. 460–467, 2012, doi: 10.1016/j.ajodo.2011.10.026.

[3] H. Lu, Y.-K. Lee, P. Villalta, J. Powers, and F. Farcia-Godoy, "Influence of the amount of UV component in daylight simulator on the color of dental composite resins," *J. Prosthet. Dent.*, vol. 96, no. 5, pp. 322–327, 2006.

[4] C. A. M. Volpato, M. R. C. Pereira, and F. S. Silva, "Fluorescence of natural teeth and restorative materials, methods for analysis and quantification: A literature review," *J. Esthet. Restor. Dent.*, vol. 30, pp. 397–407, 2018, doi: 10.1016/j.ceramint.2021.06.175.

[5] H. Matsumoto and S. Kitamura, "Applications of fluorescence microscopy to studies of dental hard tissue," *Front. Med. Biol. Engng*, vol. 10, no. 4, pp. 269–284, 2001.

[6] C. A. M. Volpato *et al.*, "Assessment of zirconia fluorescence after treatment with immersion in liquids, glass infiltration and aging," *Ceram. Int.*, vol. 47, no. April, pp. 27511–27523, 2021, doi: 10.1016/j.ceramint.2021.06.175.

[7] R. Reis *et al.*, "Evaluation of Fluorescence of Dental Composites Using Contrast Ratios to Adjacent Tooth Structure : A pilot study," *J. Esthet. Restor. Dent.*, vol. 19, no. 4, pp. 199–206, 2007, doi: 10.1111/j.1708-8240.2007.00100.x.

[8] T. Da Silva, H. De Oliveira, D. Severino, I. Balducci, M. Huhtala, and S. Gonçalves, "Direct Spectrometry : A New Alternative for Measuring the Fluorescence of Composite Resins and Dental Tissues," *Oper. Dent.*, vol. 39, no. 4, pp. 407–415, 2014, doi: 10.2341/12-464-L.

[9] C. Meller and C. Klein, "Fluorescence of composite resins: A comparison among properties of commercial shades," *Dent. Mater. J.*, vol. 34, no. 6, pp. 754–765, 2015, doi: 10.4012/dmj.2014-219.

[10] J. Kristiansen, M. Sakai, J. D. Da Silva, M. Gil, and S. Ishikawa-Nagai, "Assessment of a prototype computer colour matching system to reproduce natural tooth colour on ceramic restorations," *J. Dent.*, vol. 39, no. SUPPL. 3, pp. e45–e51, 2011, doi: 10.1016/j.jdent.2011.11.009.

[11] J. Wang, J. Lin, M. Gil, A. Seliger, J. D. Da Silva, and S. Ishikawa-Nagai, "Assessing the accuracy of computer color matching with a new dental porcelain shade system," *J. Prosthet. Dent.*, vol. 111, no. 3, pp. 247–253, 2014, doi: 10.1016/j.prosdent.2013.07.008.

[12] S. S. Mikhail and W. M. Johnston, "Confirmation of theoretical colour predictions for layering dental composite materials," *J. Dent.*, vol. 42, no. 4, pp. 419–424, 2014, doi: 10.1016/j.jdent.2014.01.008.

[13] V. Duveiller, L. Gevaux, R. Clerc, J.-P. Salomon, and M. Hebert, "Reflectance and transmittance of flowable dental resin composite predicted by the two-flux model : on the importance of analyzing the effective measurement geometry," *Color Imaging Conference 28 Proc.*, 2020.

[14] V. Duveiller *et al.*, "Predictions of the Reflectance Factor of Translucent Layered Dental Resin Composites Using Two-Flux Models: assessing the importance of the interface reflectance parameter," *CEUR Workshop Proc.*, vol. 3271, 2022.

[15] L. Simonot, M. Thoury, and J. Delaney, "Extension of the Kubelka–Munk theory for fluorescent turbid media to a nonopaque layer on a background," *J. Opt. Soc. Am. A*, vol. 28, no. 7, p. 1349, 2011, doi: 10.1364/josaa.28.001349.

[16] ISO 4049. Dentistry – Polymer-based Restorative Materials, International Organization for Standardization, 2009.

[17] CIE: Absolute methods for reflection measurements, CIE Technical Report, 1979.

[18] W. M. Johnston, N. S. Hesse, B. K. Davis, and R. R. Seghi, “Analysis of edge-losses in reflectance measurements of pigmented maxillofacial elastomer,” *J. Dent. Res.*, vol. 75, no. 2, pp. 752–760, 1996, doi: 10.1177/00220345960750020401.

[19] L. Gevaux, L. Simonot, R. Clerc, M. Gerardin, and M. Hebert, “Evaluating edge loss in the reflectance measurement of translucent materials,” *Appl. Opt.*, vol. 59, no. 28, p. 8939, 2020, doi: 10.1364/ao.403694.

[20] CIE Colorimetry, CIE technical report, 3rd Ed. (1998).

[21] P. Kubelka and F. Munk, “An article on optics of paint layers,” *Z. Tech. Phys.*, vol. 12, no. 1930, pp. 593–601, 1931.

[22] P. Kubelka, “New contributions to the optics of intensely light-scattering materials. Part I,” *J. Opt. Soc. Am.*, vol. 38, no. 5, pp. 448–457, 1948, doi: 10.1364/JOSA.38.000448.

[23] J. L. Saunderson, “Calculation of the Color of Pigmented Plastics,” *JOSA*, vol. 32, pp. 727–736, 1942.

[24] A. Gautheron, R. Clerc, V. Duveiller, L. Simonot, B. Montcel, and M. Hebert, “Light scattering in translucent layers : angular distribution and internal reflections at flat interfaces,” in Thirty Fourth Electronic Imaging Symposium: Color Imaging XXVIII: Displaying, Processing, Hardcopy, and Applications, online, 2022.

Author Biography

Vincent Duveiller is an applied photonics engineer who graduated from the Institut d'Optique Graduate School, France, in 2020. He is since enrolled in a PhD degree on the appearance reproduction using dental resin composites in the dental field at University Jean Monnet in Saint-Etienne (France), in the Hubert Curien laboratory. His research focuses on measuring optical properties of dental resin composites and improving optical models for color prediction applied to dental materials.